Offline coil position denoising enhances detection of TMS effects

Leonardo Claudino[a], Sara J Hussain[a], Ethan R Buch*[a] and Leonardo G Cohen*[a]

[a]*Human Cortical Physiology and Neurorehabilitation Section, NINDS, NIH, Building 10, Room 7D54, Bethesda, MD 20892, USA*

* These authors contributed equally to this manuscript.

Author email addresses:

leonardo.claudino@nih.gov

sara.hussain@nih.gov

ethan.buch@nih.gov

cohenl@ninds.nih.gov

Corresponding author:

Leonardo G. Cohen, M.D.

Chief, Human Cortical Physiology and Neurorehabilitation Section.

National Institute of Neurological Disorders and Stroke NIH, Building 10, Room 7D54

Bethesda, MD 20892

Ph (301) 496-9782

FAX (301) 402-7010

EMAIL. cohenl@ninds.nih.gov

HIGHLIGHTS

- Coil deviations impact TMS effects despite use of on-line neuronavigation feedback.
- Offline denoising of coil deviation impacts on TMS effects reduced variability.
- Offline denoising also significantly improved overall SNR of TMS effects.

KEYWORDS

1. TMS
2. Reproducibility
3. Neuronavigation
4. MEP
5. Corticospinal excitability

ABSTRACT

OBJECTIVE: Transcranial magnetic stimulation (TMS) is extensively used in basic and clinical neuroscience. Previous work has shown substantial residual variability in TMS effects even despite use of on-line visual feedback monitoring of coil position. Here, we aimed to evaluate if off-line modeling of coil position and orientation deviations can enhance detection of TMS effects. METHODS: Retrospective modeling was used to denoise the impact of common coil position and rotation deviations during TMS experimental sessions on motor evoked potentials (MEP) to single pulse TMS. RESULTS: Offline denoising led to a 26.19% improvement in the signal to noise ratio (SNR) of corticospinal excitability measurements. CONCLUSIONS: Offline modeling enhanced detection of TMS effects by removing variability introduced by coil deviations. SIGNIFICANCE: This approach could allow more accurate determination of TMS effects in cognitive and interventional neuroscience.

1. INTRODUCTION

Transcranial magnetic stimulation (TMS) is widely used in cognitive and interventional neuroscience (Dayan et al. , 2013). TMS effects are variable within and between individuals (Herrmann et al. , 2006, Wassermann, 2008, Pasley et al. , 2009, Nicolo et al. , 2015), as shown by the stochastic nature of motor evoked potentials (MEP) to single TMS pulses (Kiers et al. , 1993, Zarkowski et al. , 2006, Goldsworthy et al. , 2016). Sources of TMS effect variability include changes in coil position and orientation relative to the stimulation target occurring within and between experimental sessions (Mills et al. , 1992). When poorly controlled, these coil deviations are a problematic source of experimental error or noise that limits the ability to accurately measure TMS effects of interest. Stereotactic neuronavigation systems developed to address this problem provide real-time information about the position and orientation of the coil relative to the individual subject's scalp- or brain-defined target (Ruohonen et al. , 2010). To date, this information has been predominantly used to provide online visual feedback to experimenters, thus assisting in manual correction of TMS targeting errors due to coil or head movement at the time stimulation is delivered. This approach has partially improved variability in measurement of TMS effects (Lioumis et al. , 2009, Cincotta et al. , 2010, Jung et al. , 2010, Richter et al. , 2013). However, coil deviations and variable TMS effects remain present even when on-line visual feedback monitoring of coil position is implemented (Cincotta et al. , 2010, Richter et al. , 2013).

Here, we propose an offline denoising method that uses information on deviations in coil position and orientation, typically acquired by neuronavigation systems to retrospectively model and remove its impact on TMS effects. Our aim is to remove

outcome measure variance explained only by coil position and orientation deviations not resolved even despite the use of online monitoring.

2. METHODS

2.1 Participants

19 healthy adults participated in this study (13M, 6F; age=30±7.1yrs, range=22–48yrs). Subjects provided written informed consent and the study was approved by the NIH Combined Neuroscience IRB. Healthy status was verified prior to study participation via neurological examination and brain MRI performed by trained clinicians.

2.2 TMS and recording

Subjects were seated in an armchair during the study. Monophasic TMS was delivered with a hand-held figure-of-eight coil (oriented approximately 45^{o} relative to the mid-sagittal line) attached to a Magstim 200^{2} unit (Magstim, Inc). Electromyography (EMG) was recorded at 5kHz using Signal software (CED, Cambridge UK) from the left first dorsal interosseous (FDI) using disposable adhesive electrodes arranged in a belly-tendon montage. The left FDI hotspot was defined as the scalp position most reliably eliciting the largest MEPs following suprathreshold stimulation. The resting motor threshold (RMT) was defined using an adaptive threshold-hunting algorithm (Awiszus, 2003). A total of 600 suprathreshold TMS stimuli (120% RMT; interstimulus interval=5±0.75s) were then delivered to the FDI hotspot.

2.3 Neuronavigation

Frameless stereotactic neuronavigation (Brainsight 2, Rogue Research) was used to localize subject head, FDI hotspot target, and TMS coil position and orientation within the same spatial reference frame. Real-time visual feedback of the TMS coil position and orientation relative to the FDI hotspot target was used to guide hand-held TMS coil positioning over the course of the experimental session. The coil position and orientation deviations (i.e. – spatial and rotational disparity between coil and FDI hotspot target location) were acquired at the time of TMS delivery for each trial (Fig.1).

2.4 Data Analysis

2.4.1 MEP amplitudes

Peak-to-peak motor evoked potentials (MEP) amplitudes were calculated as the difference between the maximum and minimum voltage deflections between 20–40ms post-stimulus. Subjects whose mean MEP amplitudes were within one standard deviation of the grand mean were included in the analysis to avoid outlier-driven model fits (17 of 19 subjects). For a given subject, we excluded trials deemed to have excessive background EMG activity (average pre-stimulus power exceeding 75th percentile + 3*IQR over all trials). Finally, three trials with extraordinarily high x-axis coil deviations (x>35 mm compared with the grand mean, x=-0.28mm) were discovered via manual inspection and discarded.

Each 6-D coil position (x, y and z) and orientation (yaw, pitch and roll) deviation coordinate was first normalized by the maximum value across trials. Next, to increase the density of MEP amplitudes per deviation coordinate value, we independently re-quantized each

coordinate into a number of bins by using a brute-force optimization process over a range of possible number of bins (1 to 1000) that maximized detection of significant changes in MEP amplitudes with respect to the bin that included coordinate 0 (no deviation; Sign test, $p<0.05$, Bonferroni-corrected).

2.4.2 Denoising

The relationship between the coil deviations (relative to the FDI hotspot target) and MEP amplitude was modeled on a trial-by-trial basis using a mixed effects model with random intercepts at the subject level (Model 1):

$$Y = \beta_0 + X(\beta_{neg} + \beta_{pos}) + w + \epsilon \quad (1)$$

where $Y_{T\text{x}1}$ is the matrix with all T trials, $X_{T\text{x}6}$ is the design matrix of fixed effects with each row consisting of all 6-D coil deviations for each trial. We used a piecewise linear model centered at 0 to account for directional contributions of coil deviations to MEP amplitudes, represented as the fixed-effect slopes, β_{neg} and β_{pos}. Vector, w, is the individual subject mean MEP with respect to the grand mean MEP, β_0. Residuals, ϵ, are assumed to be Gaussian-distributed with zero-mean and unknown variance.

Since w reflects *any* between-subjects difference and not just those differences explained by coil deviations, a second piecewise multiple linear regression was used to obtain the fraction of between-subjects differences accounted for by *only* coil deviations (Model 2):

$$w^* = \beta_{w_0} + X^*(\beta_{w_{neg}} + \beta_{w_{pos}}) + \epsilon_w \quad (2)$$

where w^* represents the between-subjects difference explained by coil deviations. X^*represents the individual subject median coil deviations reduced to K dimensions (full 6-D coil deviation model is too high-dimensional given current sample size, N=17), via singular value decomposition (SVD):

$$X^* = [US]_{1:K} ,$$

$$\bar{X} = USV^T$$

where $\bar{X}$ represents the demeaned subject median 6-D coil deviations across trials. X^* is obtained by projecting $\bar{X}$onto the linear subspace spanned by the first K singular vectors of *V* that explained at least 90% of the original variance in $\bar{X}$ (for these data, K=3). Thus, this procedure reduced dimensionality of the acquired data by half.

Residuals ϵ_w are assumed to be normal with zero-mean and unknown variance. Slopes $\beta_{[w_{neg},w_{pos}]}$ represent the contribution of individual subject median coil deviations to the between-subject MEP difference at negative and positive values of these angles, relative to the intercept β_{w_0}.

The impact of coil deviations on MEP amplitude variability was hierarchically decomposed into terms expressing MEP variability explained by both within-subject/trial-to-trial (lower level) and between-subject (higher level) factors, by substituting *w* in Eq.1 with w^* (Eq.2).

$$Y = \beta_0 + X(\beta_{neg} + \beta_{pos}) + \beta_{w_0} + X^*\left(\beta_{w_{neg}} + \beta_{w_{pos}}\right) + \epsilon_w + \epsilon\,.$$

Finally, denoised MEP amplitude estimates, $\hat{Y}$, were obtained by subtracting the total fraction of MEP variability explained by coil deviations:

$$\hat{Y} = Y - X(\beta_{neg} + \beta_{pos}) - X^*(\beta_{w_{neg}} + \beta_{w_{pos}}). \quad (3)$$

2.4.3 Assessment of denoising

We assess the effect of denoising as percent changes in mean, variance and signal-to-noise ratio from raw (Y) to denoised ($\hat{Y}$) MEP amplitudes between all trials of all subjects:

$$\Delta F_{all} = \frac{F(\hat{Y})}{F(Y)} - 1$$

and as the median change within each subject *s*:

$$\Delta F_s = median_s\left(\frac{F(\hat{Y}_s)}{F(Y_s)} - 1\right)$$

where *F* is one of the following functions: variance (*Var*), mean (*Mean*) or signal-to-noise ratio (*SNR*). Y_s and $\hat{Y}_s$ are the individual subject, s, subsets of raw and denoised MEP amplitudes, respectively.

3. RESULTS

The main result was that offline denoising led to a significant improvement in SNR of corticospinal excitability measurements (Fig.2).

Despite online monitoring, the actual coil position and orientation varied substantially with respect to the target hotspot (range of -4.87–3.89mm and -0.27–0.36rad or -15.42^{o}–20.53^{o}, respectively; Fig.1c). Offline modeling of the impact of these residual coil deviations corrected this source of individual-trial, MEP amplitude measurement error. Specifically, denoising significantly increased within-subject mean MEP amplitudes ($\Delta Mean_{WS}$=24.23%, V=140, p=0.0007) without affecting the variance (ΔVar_{WS}=-1.80%, V=53, p=0.142), overall resulting in a significant improvement in signal-to-noise ratio (ΔSNR_{WS}=26.19%, V=141, p=.0005; Fig.2b).

Across-subjects, denoising decreased MEP amplitude variance over trials (random permutation test 20,000 repetitions, ΔVar_{all}=6.99%, p=0.00005) in the absence of mean or signal-to-noise ratios changes ($\Delta Mean_{all}$=18.28%, p=0.366 and ΔSNR_{all}=22.64%, p=0.271 respectively).

4. DISCUSSION

The main finding of this study was that retrospective modeling of coil position and orientation deviations improved MEP amplitude measurement SNR by 26.19%.

MEP amplitudes are widely used as outcome measures or as a strategy to standardize TMS stimulation intensity across individuals in systems, cognitive and clinical neuroscience (Herbsman et al. , 2009, Kaminski et al. , 2011). Here, we used coil position and orientation deviation information saved after customary online monitoring to

subsequently characterize MEP amplitude variability explained only by uncontrolled coil deviations, and then denoise MEP measurements offline. These data are usually available, but commonly unused in statistical analysis pipelines after data is collected.

The improvement in SNR identified here raises the possibility of substantial enhancement of TMS effect detection through offline, coil deviation-based denoising. Theoretically, this approach could be applied to both previously acquired data and future studies as a means to more accurately measure trial-by-trial motor thresholds and other neurophysiological features (i.e., intracortical inhibition or facilitation, recruitment curves, and transcranial evoked potentials)(Hallett, 2007, Lioumis et al. , 2009), or behavioral TMS effects (i.e., single pulse TMS effects on reaction times)(Chen et al. , 1998, Johansen-Berg et al. , 2002). This approach could also be extended to denoise cumulative effects of repetitive TMS neuromodulation sessions (i.e. – 1Hz rTMS) on neurophysiological measures (Chen et al. , 1997) or behavior (Censor et al. , 2010). Finally, this methodology is likely to be particularly useful for study designs that include pre- and post-intervention measurements, multiple sessions for a single subject, or multiple operators across different centers)(Julkunen et al. , 2009, Fleming et al. , 2012).

5. CONCLUSIONS

Offline denoising may be a simple and feasible approach to enhance detection of TMS effects in systems neuroscience.

CONFLICT OF INTEREST STATEMENT

None of the authors have potential conflicts of interest to be disclosed.

ACKNOWLEDGMENTS

This work was supported by the Intramural Research Program of the National Institute of Neurological Disorders and Stroke.

REFERENCES

Awiszus F. TMS and threshold hunting. Suppl Clin Neurophysiol. 2003;56:13-23.

Censor N, Dimyan MA, Cohen LG. Modification of existing human motor memories is enabled by primary cortical processing during memory reactivation. Curr Biol. 2010;20:1545-9.

Chen R, Classen J, Gerloff C, Celnik P, Wassermann EM, Hallett M, et al. Depression of motor cortex excitability by low-frequency transcranial magnetic stimulation. Neurology. 1997;48:1398-403.

Chen R, Yaseen Z, Cohen LG, Hallett M. Time course of corticospinal excitability in reaction time and self-paced movements. Ann Neurol. 1998;44:317-25.

Cincotta M, Giovannelli F, Borgheresi A, Balestrieri F, Toscani L, Zaccara G, et al. Optically tracked neuronavigation increases the stability of hand-held focal coil positioning: evidence from "transcranial" magnetic stimulation-induced electrical field measurements. Brain Stimul. 2010;3:119-23.

Dayan E, Censor N, Buch ER, Sandrini M, Cohen LG. Noninvasive brain stimulation: from physiology to network dynamics and back. Nat Neurosci. 2013;16:838-44.

Fleming MK, Sorinola IO, Newham DJ, Roberts-Lewis SF, Bergmann JH. The effect of coil type and navigation on the reliability of transcranial magnetic stimulation. IEEE Trans Neural Syst Rehabil Eng. 2012;20:617-25.

Goldsworthy MR, Hordacre B, Ridding MC. Minimum number of trials required for within- and between-session reliability of TMS measures of corticospinal excitability. Neuroscience. 2016;320:205-9.

Hallett M. Transcranial magnetic stimulation: a primer. Neuron. 2007;55:187-99.

Herbsman T, Forster L, Molnar C, Dougherty R, Christie D, Koola J, et al. Motor threshold in transcranial magnetic stimulation: the impact of white matter fiber orientation and skull-to-cortex distance. Hum Brain Mapp. 2009;30:2044-55.

Herrmann LL, Ebmeier KP. Factors modifying the efficacy of transcranial magnetic stimulation in the treatment of depression: a review. J Clin Psychiatry. 2006;67:1870-6.

Johansen-Berg H, Rushworth MF, Bogdanovic MD, Kischka U, Wimalaratna S, Matthews PM. The role of ipsilateral premotor cortex in hand movement after stroke. Proc Natl Acad Sci U S A. 2002;99:14518-23.

Julkunen P, Saisanen L, Danner N, Niskanen E, Hukkanen T, Mervaala E, et al. Comparison of navigated and non-navigated transcranial magnetic stimulation for motor cortex mapping, motor threshold and motor evoked potentials. Neuroimage. 2009;44:790-5.

Jung NH, Delvendahl I, Kuhnke NG, Hauschke D, Stolle S, Mall V. Navigated transcranial magnetic stimulation does not decrease the variability of motor-evoked potentials. Brain Stimul. 2010;3:87-94.

Kaminski JA, Korb FM, Villringer A, Ott DV. Transcranial magnetic stimulation intensities in cognitive paradigms. PLoS One. 2011;6:e24836.

Kiers L, Cros D, Chiappa KH, Fang J. Variability of motor potentials evoked by transcranial magnetic stimulation. Electroencephalogr Clin Neurophysiol. 1993;89:415-23.

Lioumis P, Kicic D, Savolainen P, Makela JP, Kahkonen S. Reproducibility of TMS-Evoked EEG responses. Hum Brain Mapp. 2009;30:1387-96.

Mills KR, Boniface SJ, Schubert M. Magnetic brain stimulation with a double coil: the importance of coil orientation. Electroencephalogr Clin Neurophysiol. 1992;85:17-21.

Nicolo P, Ptak R, Guggisberg AG. Variability of behavioural responses to transcranial magnetic stimulation: Origins and predictors. Neuropsychologia. 2015;74:137-44.

Pasley BN, Allen EA, Freeman RD. State-dependent variability of neuronal responses to transcranial magnetic stimulation of the visual cortex. Neuron. 2009;62:291-303.

Richter L, Trillenberg P, Schweikard A, Schlaefer A. Stimulus intensity for hand held and robotic transcranial magnetic stimulation. Brain Stimul. 2013;6:315-21.

Ruohonen J, Karhu J. Navigated transcranial magnetic stimulation. Neurophysiol Clin. 2010;40:7-17.

Wassermann EM. The Oxford handbook of transcranial stimulation. Oxford ; New York: Oxford University Press; 2008.

Zarkowski P, Shin CJ, Dang T, Russo J, Avery D. EEG and the variance of motor evoked potential amplitude. Clin EEG Neurosci. 2006;37:247-51.

FIGURE 1

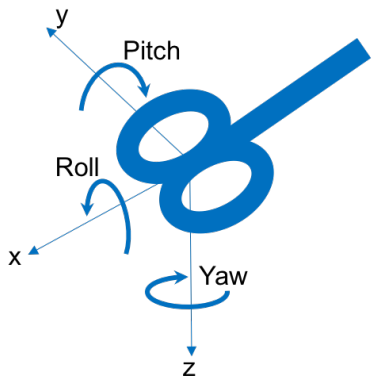

(A)

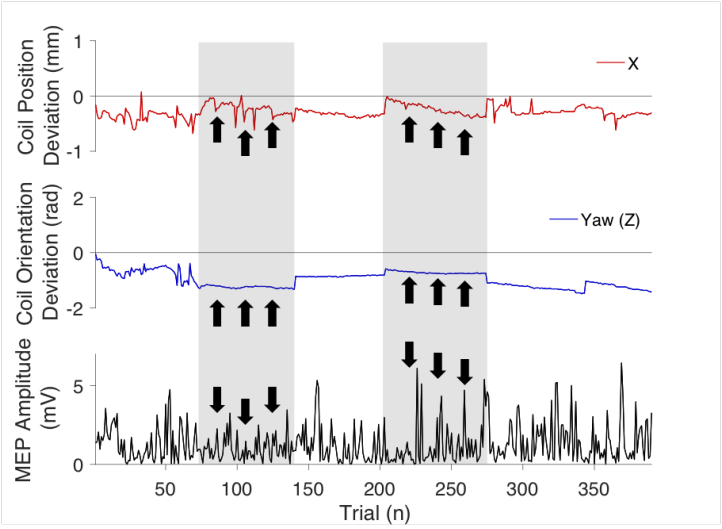

(B)

FIGURE 2

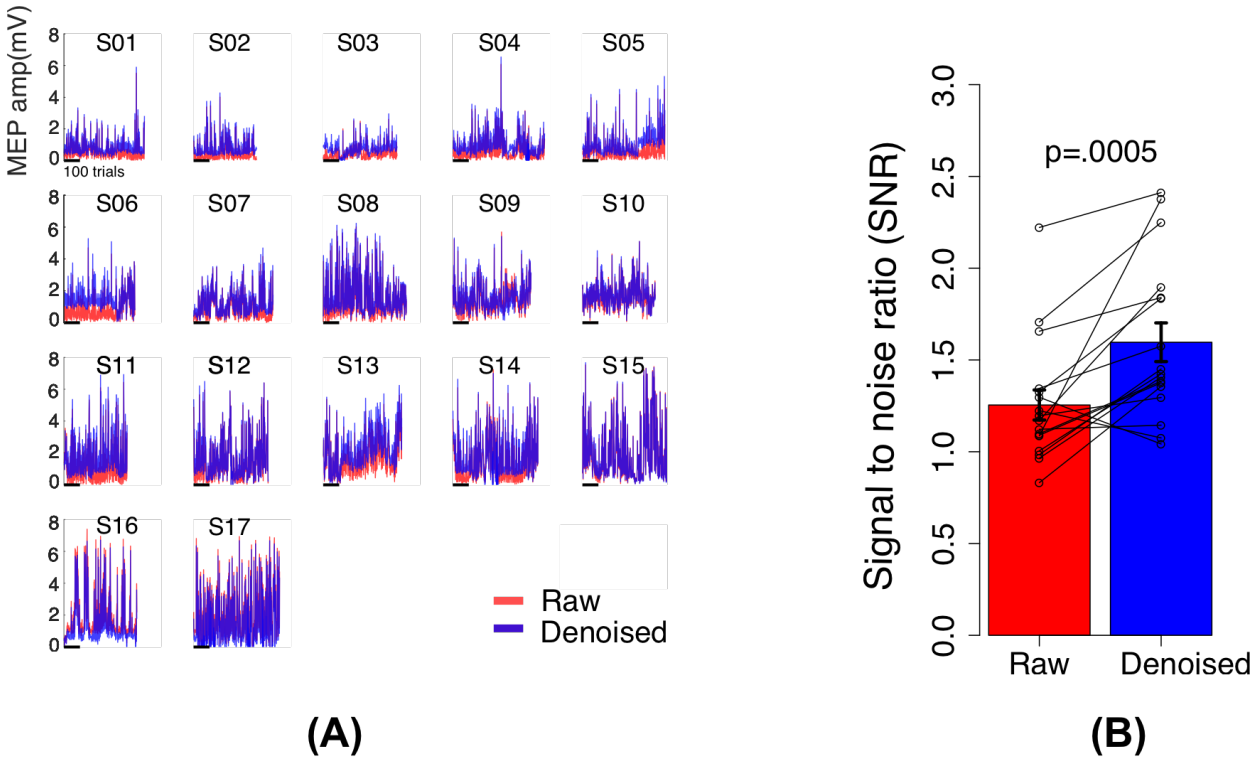

FIGURE CAPTIONS

Figure 1. (A) Coil position and orientation. For each TMS pulse, the neuronavigation software recorded the displacement of the coil with respect to the target scalp location as a homogeneous transformation matrix (rotations and translations). Later, as part of the offline analysis, these matrices are condensed into spatial (x, y and z) and rotational (roll, pitch, yaw) coordinates, as depicted. (B) Correlated changes in coil position and orientation deviations, and MEP amplitudes for one representative subject. Coil deviation and MEP amplitude data for each trial is shown over the course one experiment. For visualization purposes, only the x-axis position and yaw (z-axis) orientation deviation coordinates are shown for the coil data. The shaded grey area to the left shows a period in the experiment where coil position deviations along the x-axis change sharply from trial-to-trial, while the yaw orientation deviation shows a constant negative shift away from the stimulation target. MEP amplitudes show a corresponding mean decrease relative to trials before and after this period consistent with the orientation deviation shift, along with local fluctuations largely consistent with the x-axis position deviations. A different patter of coil position and orientations is show in the shaded area on the right, with gradual linear drifts away from the target occurring along both x-axis position and yaw orientation coil deviation dimensions. MEP amplitudes decay throughout this period in a similar manner. Other coil deviation dimensions or factors unrelated to coil deviations could explain the initial reduction in MEP amplitudes over the first several trials of this period.

Figure 2. (A) Raw and denoised peak-to-peak MEP amplitudes in all trials and subjects. Each plot corresponds to a subject (S01 to S17) with the ordinate depicting absolute peak-to-peak MEP amplitudes. The dark bar in the abscissa represents a scale of 100 trials. Red and blue lines represent raw and denoised MEP amplitudes. (B) Retrospective coil related variance denoising improved the signal to noise ratio in MEP amplitude determination by 26.19% (p=.0005).